TRANSVERSE REINFORCEMENT EFFECTS ON ANCHORED DEFORMED BARS

Giovanni A. Plizzari
Professor

Massimo A. Deldossi
Structural Engineer

Stefano Massimo
Structural Engineer

Dept. of Civil Engineering
University of Brescia - Via Branze, 38 - Brescia 25123 - Italy
email:plizzari@bsing.ing.unibs.it

Published on:
Magazine of Concrete, Vol.50(2), pp. 161-177

April 4, 2002

1 Introduction

In anchorages and lap splices of large diameter ribbed bars, because of the wedge action of the ribs, splitting cracks are often present in the concrete surrounding the bar [1]. These cracks start from flexural cracks, where the bar-to-concrete slip reaches its maximum, and propagate in longitudinal planes along the reinforcing bar (Fig. 1). Splitting cracks may also be present along the transfer zones of prestressing strands owing to the transverse deformation of the tendon.

Splitting cracks impair bond mechanical behaviour (stiffness and strength) and make bond sensitive to confinement [2]. They also have particular relevance for structural durability owing to their longitudinal propagation that exposes a large area of the bar to the environment; this should make the corrosion resistance of members with splitting cracks lower than the resistance of members with flexural cracks [3].

After splitting, the confining action along anchored bars or splices is partly produced by transverse reinforcement [1, 4, 5], by concrete tensile strength in the uncracked cover and by concrete cohesive stresses between the crack faces in the split cover [1, 6, 7, 8]. Moreover, where it is present, an external transverse pressure provides a further confining action [2, 9, 10] (Fig. 2a).

In beams with small concrete cover and clear spacing between the rebars, transverse reinforcement provides the most relevant confining action, especially in zones far from direct supports where external pressure is not present. If transverse reinforcement is not sufficient, splitting cracks open and develop abruptly along the anchored bars and a sudden anchorage collapse occurs [1, 4, 11] ("splitting failure", Fig. 2b); on the contrary, an adequate number of stirrups limits splitting crack opening and allows the bond stress to increase until the compressive failure of the concrete layer around the ribs occurs ("pull-out failure"; Fig. 2c).

Anchorage behaviour can be correctly studied only if splitting and confinement are taken into account [12]. The research-work on concrete splitting available in the literature mainly regards the bond behaviour in short anchorages. A theoretical model, valid in the influence zone of one stirrup, was proposed in [11]; it provides relationships between bond stress, bar-to-concrete slip, splitting crack opening and stirrup stress. As far as long anchorages are concerned, the numerous experimental results available mostly give information on the overall anchorage capacity but little on splitting crack opening and development [13, 14], so that several aspects related to splitting in anchorage behaviour still need to be investigated.

Because of the complexity of the mechanical aspects involved, the study of anchorage behaviour requires further basic tests to shed new light on the development of splitting cracks along the bars. To this end, in the present research-work long anchorages with transverse reinforcement were tested with the aim of studying the confining effects of stirrups. Particular attention was devoted to gathering more detailed results on splitting crack propagation along the anchored bar and on stirrup stresses, in order to provide needed information for further theoretical modelling. Moreover, a relationship between the anchorage capacity and the amount of transverse reinforcement is determined and a comparison is made with the values proposed in the building codes [15, 16].

The experiments concern pull-out tests, which are certainly one of the simplest ways to test anchorages but are often influenced by the confining action provoked by the friction between the specimen and the contrast plate. This friction becomes particularly important when long anchorages are tested, because of the higher pull-out loads involved. In order to eliminate this confining action, which is not found in any actual structure, a special set-up was adopted.

2 Test planning and materials

2.1 Specimen geometry

The specimens concerned two anchored bars with three two-legged stirrups. They simulate a concrete block close to a flexural crack at an indirect support (where transverse pressure is not present) and plane BB ideally represents one crack face (Fig. 1). The concrete block embedding the bars is somewhat simplified and is cast as a thick plate with two bars laying in mean plane AA. The anchored bars had a diameter, ϕ_p, of 20 mm and an embedment length, l_b, of 450 mm; consequently, the stirrup spacing distance (Δz) was 150 mm (Fig. 3b). The stirrups had different diameters (ϕ_{st}) with the purpose of studying the anchorage response for different amounts of transverse reinforcement; in order to measure the confining contribution of the concrete cover and the clear spacing between the bars, two specimens had no stirrups (Table 1).

With closely-spaced anchored bars, concrete tends to split in the plane containing the bars (Fig. 1). In order to reproduce this case and to provoke the maximum force in the transverse reinforcement, a small specimen width was chosen (b= 120 mm); furthermore, the principal bars were placed with the ribs acting at right angles to the plane passing through the bar axes so that plane AA became the preferential plane for the formation of the splitting crack (Figs. 3b,c). The stirrup ribs were oriented in to avoid wedge actions towards the concrete surface. The anchored bars were machined to remove the ribs in the first 25 mm of the bar at each end of the concrete block so that these bar ends were made unbonded. Two steel angles placed in the concrete preformed a splitting crack in plane AA (Figs. 3a,b).

As far as anchorages in split concrete are concerned, the following two significant parameters should be considered [11]:

- "stirrup index of confinement" Ω, defined as the ratio between the total area of stirrups $n_{st}A_{st}$ and the total area of the longitudinal section of the anchored bars $n_pA_p^*$ in the influence zone Δz of one stirrup:

$$\Omega = \frac{n_{st}A_{st}}{n_pA_p^*} = \frac{n_{st}\pi\phi_{st}^2}{4n_p\phi_p\Delta z} \tag{1}$$

  where n_p is the number of anchored bars and n_{st} is the number of stirrup legs;

- "concrete index of confinement" B, defined as the ratio between the net area of concrete in Δz and $n_pA_p^*$:

$$B = \frac{(b - n_p\phi_p)\Delta z}{n_p\phi_p\Delta z} \tag{2}$$

where b is the specimen (or beam) width.

The values of Ω for the specimens tested are shown in Table 1; the small specimen width corresponds to a value B=2 for all the specimens.

2.2 Instrumentation

The instrumentation consisted of a set of strain gauges and LVDTs (Linear Variable Differential Transformers). The former allowed the determination of the stirrup and the principal bar stresses; the latter were adopted to measure splitting crack opening close to the stirrups as well as the bar slip at both loaded and unloaded ends (Fig. 3).

Slip δ_L at the loaded end of the bars was measured by means of two transducers (at each bar) to take possible bar rotations into account (Fig. 3b). Since the aluminum support on the anchored bar was placed at a distance of about 95 mm from the beginning of the embedded zone, slip δ_L was determined by subtracting the elastic elongation of the bar from the measured displacement δ=$(\delta_1 + \delta_2)/2$. Slip δ_F at the free end of the bars was measured by means of one LVDT placed on the concrete surface close to the bar.

The splitting crack opening close to the stirrups was measured by six LVDTs attached to small aluminum supports glued to the specimen at a distance of about 60 mm (Fig. 3). Since the elastic deformation along the short base length after cracking is negligible, the measurements provide the splitting crack opening.

Strain gauges were placed outside the embedment length of the principal bars and in the middle section of some stirrups (Figs. 3a,c); the effective area of the weakened section of the stirrups was determined by measuring the load-strain relationship (in the middle section) before casting, and assuming a Young's modulus for steel of 206.000 MPa (Table 1).

Splitting crack propagation was illustrated by means of a thin layer of gypsum placed on the specimen surface along the splitting plane AA (Fig. 5); the crack tip position was determined by observation by means of a magnifying glass (6x).

2.3 Experimental set-up and loading modalities

As mentioned above, in split concrete, bond is strongly dependent on the confining action present along the bar. While the confining action developed by both concrete cover and transverse reinforcement are often found in actual structures, the friction-induced confining action at the loaded end of pull-out specimens is only related to the test set-up, it varies during the experiment and also is different in different tests. In order to avoid this confining action, a special (and simple) fixture, based on a concept previously proposed by Giuriani and Plizzari [5], was adopted here. In this fixture, the pull-out force acting on the specimen was counteracted by two bottom plates, separated along the main splitting plane (AA) (Figs. 3 and 4). The contrast plates were connected to the upper part of the fixture by means of four bars with bolts which do not have any flexural stiffness so that concrete blocks C1 and C2 are allowed to move freely (Fig. 4).

The fixture was assembled in an Instron 2714/8500 hydraulic servo-controlled test machine. The signal from the LVDT of the actuator was used as the control parameter. The load was applied by imposing a continuous displacement of the actuator up to a maximum loaded-end slip of 4-5 mm (about half the distance between the ribs). The average displacement rate was 20 μm/min; because of the elastic deformation of the fixture, the bar-to-concrete slip rate was even smaller, so that the specimens could be considered as subjected to a quasi-static loading process. The load applied from the machine was measured by a reversible load cell with a capacity of 250 kN and a sensitivity of 0.025 kN/mV; this measurement allowed for a double check of the load determined by means of the strain gauges applied to the anchored bars. During the test, some unloading and reloading cycles were performed.

The measurements from the strain gauges and LVDTs were converted from analog to digital by an HBM UPM 100 multipoint measuring unit, and then stored in a PC at a frequency of 1 Hz.

Further details about the experimental set-up can be found in [17].

3 Material properties

The concrete mix proportions are the following:

- Portland cement Type II 32.5 A/L-R: Portland: 325 kg/m^3;
- water: 175 l/m^3 (water-cement ratio = 0.54);
- aggregates (sand and river gravel): 1853 kg/m^3 (see also Table 2);
- superplasticizer: 3.3 l/m^3.

The application of strain gauges required machining the anchored bars in order to have a smoother surface; in doing so, the bar section was somewhat reduced where the strain gauges were placed. The weakening of the section is more significant for *Tempcore*© bars, which are characterized by a stronger outer shell. Albeit there are no detrimental effects on short anchorages, a certain reduction in load capacity has to be expected in long anchorages because of the earlier yielding of the bar in the weaker sections, as occurred in the first tests performed. In order to avoid the reduction of the maximum pull-out load, a special heat treatment was applied to the bars to increase the yield strength of the bar to about 1200 MPa, without changing the other mechanical properties (Table 3).

The stirrups having a 5 mm diameter were cold-drawn steel bars, while all the other stirrups, as well as the principal bars, were hot-rolled bars; their geometrical and mechanical properties are shown in Table 3.

The concrete was poured into wood forms with the principal bars in a vertical position (Fig. 3b); since the casting direction was the opposite of the pull-out force, better bond characteristics were obtained [18]. Two days after casting, the specimens were demoulded and then cured in water until two weeks before the test; then they were stored in the laboratory at 15-25^oC and ≈70% R.H. The workability of the fresh concrete, measured on the different batches with a typical slump test, varied between 100 and 140 mm. During the pour, six sample cylinders (ϕ x h = 100 x 300 mm) and two cubes (a=150 mm) for each specimen, were cast and cured in the same manner as the specimens. After 28 days of curing, compressive strength $f_{c,28}$, (direct) tensile strength $f_{ct,28}$ and Young's modulus $E_{c,28}$ were measured on the cylinders; the values obtained are summarized in Table 4. Before each test, concrete compressive strength $f_{c,cube}$ was determined by testing of the cubes (Table 5).

4 Results and Discussion

In all specimens, owing to the presence of the preformed crack between the steel angles at the loaded end of the specimen and to the orientation of the bar ribs, a main splitting crack formed along plane AA (Figs. 3b and 5a). In some specimens secondary splitting cracks appeared in other longitudinal planes (generally after the peak load) [17]. The main splitting crack allowed the transverse reinforcement to work properly, since it was at right angles to the split-concrete faces.

Figure 6 exhibits the typical results obtained from specimen 45S5P4, having stirrups of 5 mm. In particular, the figure shows plots of pull-out force F, splitting crack widths w_{s1}, w_{s2}, w_{s3} (measured at the stirrup levels), stress σ_{s1}, σ_{s2} and σ_{s3} in the first, second and third stirrup (from the loaded end of the bar), and free-end slip δ_F, as functions of loaded-end slip δ_L (the results are plotted both up to the maximum slip and up to the peak load and concern the left and the right sides of the specimen). Notice the two unloading and reloading cycles performed during the test, when the tensile stress in the anchored bar was about 150 and 240 MPa respectively.

The values of maximum load F_{max}, slip at the maximum load $\delta_{L,P}$, maximum anchored bar stress σ_P (evaluated on the basis of the nominal bar diameter), maximum bond stress τ_u (assumed evenly distributed along the bar), concrete compressive strength $f_{c,cube}$ and the age of the specimens at the time of the test are summarized in Table 5. Unfortunately, because of unexpected rotations of the specimen that occurred during the tests, only one test of specimens with 10 mm diameter stirrups was successful. As mentioned above, a special heat-treated steel was adopted to avoid early yielding of the weaker sections of the anchored bar instrumented with strain gauges; however, it should be noted that observed maximum bar stress σ_P generally was lower than 550-600 MPa, which is a typical yield strength of steel often used in Europe.

The complete set of experimental results can be found in [17].

4.1 Bond-slip relationship

A comparison between the curves of the average bond stress versus loaded-end slip δ_L (normalised to ϕ_p), is shown up to the peak load in Fig. 7. Although bond capacity was found to depend on the square root of the concrete compressive strength [19], here τ_u is normalised to $f_{c,cube}$ in order to obtain dimensionless diagrams; this was possible since concrete compressive strength (determined at the time of the tests) showed a low scatter.

It should be noted that in specimens 45NSP1 and 45NSP2, without transverse reinforcement, a brittle splitting collapse of the anchorage occurred when the splitting crack reached the unloaded end of the anchored bars (Fig. 7a). In these specimens, after anchorage failure, the concrete corbels between the ribs were undamaged. In each diagram of Fig. 7, the mean curve is plotted with the experimental results; all the mean curves are then reported in Fig. 7f showing that, for increasing values of the stirrup diameter (and thus of the stirrup index of confinement), both bond stiffness and capacity increased.

4.2 Splitting-crack opening and propagation

Figure 8 exhibits splitting crack opening w_{s1} at the first stirrup level versus the principal bar stress as measured up to the peak load for all the specimens. To ease the comparison, for each stirrup diameter the mean curves were determined and plotted together in Fig. 8f. It is worth noting that the smaller the stirrup diameter is, the larger the splitting crack opening. Furthermore, splitting crack width reaches remarkable values under service loads; for example, in specimens with 5 mm stirrups, splitting crack width is nearly 0.2 mm when the principal bar stress is 250 MPa.

The splitting crack penetration Y, measured from the loaded end of the anchorage and divided by embedment length of the bar l_b, is plotted versus the normalised bond stress $\tau/f_{c,cube}$ in Fig. 9; therefore, the normalised splitting crack penetration varies from zero (splitting crack not present) to one (splitting crack completely propagated). From these results, the splitting crack length seems to increase linearly with the applied load. It should be noted that the splitting-propagation rate is lower for larger stirrup diameters and that in specimens with transverse reinforcement, the anchorage capacity was reached after the complete propagation of the splitting crack along the bar, owing to the favourable effects of the confinement action.

4.3 Stresses in transverse reinforcement

In Fig. 10 the stress in the stirrup closest to the loaded end of the bar is plotted versus the loaded-end bar slip. Unfortunately, strain gauges glued to the stirrups did not always work properly and few experimental curves are available. The stresses are determined by using the effective area of the stirrups, shown in Table 1. The large scatter of the experimental results is probably due to the irregular surfaces of the splitting cracks that often did not lay in the stirrup middle section where strain gauges were placed (Fig. 5); this resulted in experimental measurements smaller than the actual maximum stirrup stresses. All the experimental curves are plotted up to the yield stress, as determined for the different stirrups (Table 3); it can be noted that the smaller the stirrup diameter is, the higher the stirrup stress and the sooner yielding occurs. However, all the small diameter stirrups (5 and 6 mm) closest to the loaded end of the principal bars yielded before the specimens reached the maximum bond stress. In the same figure, empty squares illustrate the stirrup stress when the characteristic bond strength prescribed by Eurocode 2 ($f_{bk,EC2}$) [15] is reached; this is evaluated on the basis of the concrete compressive strength determined at the time of the tests. The filled squares indicate that the stirrup yielded before reaching $f_{bk,EC2}$. Although the transverse reinforcement amount was always higher than the minimum prescribed by Eurocode 2 ($\Omega_{min,EC2}$ ≈0.0044 for a beam with two anchored bars having ϕ_p = 20 mm and l_b = 450 mm), this occurred in all the stirrups monitored, with the exception of two specimens with ϕ_{st}=8 mm, where the stirrup stresses were higher than 400 MPa. This behaviour is more significant if one considers that, as mentioned above, the measurements did not always provide the actual maximum stress in the stirrups and that in actual structures, besides bond effects, stirrups are stressed by other actions. Therefore, stirrup stresses related to bond can reduce the ultimate structure load capacity since they can provoke an earlier stirrup failure. Moreover, in specimens with ϕ_{st}=5 mm, the stirrups yielded when the loaded-end slip was about 0.4 mm, and the principal-bar stress was about 260 MPa, which is typical of bar stresses under service loads.

4.4 Anchorage capacity

Figure 11a exhibits the ultimate bond stress τ_u versus the stirrup index of confinement Ω (Eq. 1), as obtained from all the specimens tested; in this diagram, the bond strength is normalised to the concrete compressive strength $f_{c,cube}$ determined at the time of the test (Table 5). In the same figure, the results obtained by the authors in previous tests are also plotted (Series 1 [14]). It can be observed that bond capacity increases with the stirrup index of confinement and tends to an upper bound that is reached for a value $\Omega \approx 0.03 - 0.04$; beyond this value, no significant increase of bond strength occurs. It is worth mentioning that the specimens of the previous tests [14] were characterized by different values of the "concrete index of confinement" B; however, small values of this index do not significantly influence the anchorage capacity of rebars in normal concrete [14, 20], so that the results should be comparable. An increase of anchorage capacity of transversely-reinforced rebars was also observed by Morita and Fujii [21], by Kaku and co-workers [22, 23] and by Maeda and co-workers [20], by testing beam specimens with 19 mm diameter flexural reinforcement. Figure 11b shows some of these results referring to the average response of corner bars ("supported" by 90^o stirrup corner bends) and inner bars ("unsupported"); the latter are characterized by a lower anchorage capacity owing to the larger splitting crack opening that locally occurs [21]. These different restraints would explain the lower values of bond strength of Fig. 11b with respect to the ones of Fig. 11a, since the two anchored bars of the present series of tests were better confined being both "supported" by stirrup legs (Fig. 3). The lower effectiveness of stirrups in restraining interior ("unsupported") bars was already observed by Warren [24] who tested specimens containing from two to seven bars within a single two-legges stirrup [25]. This again underlines the importance that a correct transverse-reinforcement placement has on anchorage capacity owing to the different splitting crack development along the section width [14]. Experimental results of Fig. 11 do not show any upper bound but the experiments regarded specimens with $\Omega \leq 0.035$.

4.5 Code provisions

In this section, the provisions for anchorages of Eurocode 2 (EC2) [15] and ACI 318-95 [16] are compared with the experimental results. These provisions mainly regard the anchorage capacity and do not refer to the splitting crack related durability [3].

According to Eurocode 2 [15], the anchorage length can be determined by assuming a constant bond stress along the bar $f_{b,EC2}$ which can be expressed as:

$$f_{b,EC2} = \frac{f_{bk,EC2}}{\gamma_c} = \frac{0.4275 f_{ck}^{2/3}}{\gamma_c} \tag{3}$$

where γ_c (=1.5) is the safety factor for concrete and $f_{b,EC2}$ as well as f_{ck} are expressed in MPa. It can be noted that $f_{b,EC2}$ is independent of the transverse reinforcement present along the bar; EC2 only requires a minimum amount of stirrups that, for a beam similar to the tested specimens (Figs. 1 and 3), corresponds to $\Omega_{min,EC2} \approx 0.0044$.

The ACI 318-95 code [16] prescribes a development length that, for normal concrete and good bond conditions, is given by:

$$\frac{l_b}{\phi_p} = \frac{3}{40} \frac{f_y}{\sqrt{f'_c}} \frac{\gamma}{\left(\frac{c}{\phi_p} + \frac{K_{tr}}{\phi_p}\right)} \tag{4}$$

where $\gamma = 0.8$ for No. 6 ($\phi_p \leq 19$ mm) and smaller bars and $\gamma = 1.0$ for all other bars, f_y is the specified yield strength of reinforcement, f'_c is the specified cylinder compressive strength of concrete, c is the smaller of either the distance from the center of the bar to the nearest concrete surface or one half the center-to-center spacing of the bars. K_{tr} is the *transverse reinforcement index* which is given by:

$$\frac{K_{tr}}{\phi_p} = \frac{n_{st} A_{st} f_{yt}}{1500 \phi_p \Delta z n_p} \tag{5}$$

where f_{yt} is the specified yield strength of transverse reinforcement. The term in the denominator of Eq. 4 that takes into account the confining action provided by concrete cover and transverse reinforcement, has the limitation:

$$(\frac{c}{\phi_p} + \frac{K_{tr}}{\phi_p}) \leq 2.5 \tag{6}$$

Note that Eqs. 4 and 5 are valid for stresses expressed in psi. K_{tr} is a coefficient similar to the stirrup index of confinement Ω (Eq. 1); in fact, it can be written as:

$$\frac{K_{tr}}{\phi_p} = \Omega \frac{f_{yt}}{1500} \tag{7}$$

By assuming a uniform bond stress distribution along the bar and expressing the stresses in MPa, the bond strength according to ACI 318-95 becomes:

$$f_{b,ACI} = \frac{f_y \phi_p}{4 l_b} = \frac{0.277\sqrt{f_c'}}{\gamma}(\frac{c}{\phi_p} + 0.0967 \Omega f_{yt}) \tag{8}$$

and the limitation of Eq. 6 can be written as:

$$\Omega \leq \Omega_{max,ACI} = (2.5 - \frac{c}{\phi_p})\frac{10.34}{f_{yt}} \tag{9}$$

It is worth noting that the bond strength according to ACI is linearly dependent on the concrete cover (or on the clear spacing between the bars) [25, 26], and on the stirrup index of confinement, up to a value $\Omega_{max,ACI}$ beyond which a constant bond strength should be adopted.

A linear dependency of bond capacity on the transverse reinforcement area has been observed by Morita and Fujii [21], by Darwin and coworkers [27] and by Orangun et al. [25] who proposed a bilinear approximation to take the upper bound of the bond strength into account. The linear increase of bond capacity versus the confining action was also observed by Gambarova and Rosati [28] and Modena and co-workers [29] who did pull-out tests on reinforcement in concrete blocks with external transverse pressure.

The bond strength as prescribed by Eurocode 2 and ACI 318-95 is plotted as a function of Ω in Fig. 11 along with the experimental results. Bond strengths $f_{b,EC2}$ and $f_{b,ACI}$

were determined by assuming the following values of the mechanical properties and of the geometrical characteristics, which are similar to those of the experiments shown in Fig. 11: $f_{yt} = 500$ MPa, $f_{ck} = f'_c = 25$ MPa (that, according to code [15], corresponds to $f_{ck,cube} = 30$ MPa), $\gamma = 1.0$ for the results plotted in Fig. 11a ($\phi_p = 20$ mm) and $\gamma = 0.8$ for the results shown in Fig. 11b ($\phi_p = 19$ mm), and $c/\phi_p = 1.5$. The latter is evaluated from the geometry of the specimens tested in the present research-work but also averages the values of the specimens tested in [14, 20, 22, 23] that vary between 1.25 and 2.5. Based on the adopted mechanical properties of materials and parameter c/ϕ_p, a value $\Omega_{max,ACI} = 0.0208$ was obtained. It is worth noting that $f_{b,EC2}$ approaches the experimental results for small values of Ω (close to the small amount required) and remarkably underestimates the experimental results when a larger amount of transverse reinforcement is adopted (Fig. 11a). The bond strength prescribed by ACI is closer to the experimental trend owing to the linear increase with Ω, but it also remarkably underestimates the bond capacity for large amounts of transverse reinforcement ($\Omega > 0.03$). However, when bars are "unsupported" by stirrups so that a larger splitting crack opening occurs, $f_{b,EC2}$ as well as $f_{b,ACI}$ overestimate some of the experimental results obtained in [20, 22, 23] (Fig. 11b).

5 Conclusions

Pull-out specimens with long anchorages of ribbed bars confined with stirrups were tested with the aim of studying the confining effects of transverse reinforcement on splitting crack development and anchorage behaviour. A special test set-up allowed to eliminate the confining action due to friction at the counteracting plate to better simulate an actual structure.

The experimental results can be summarized as follows:

- The maximum splitting crack opening increased for decreasing transverse-reinforcement diameter size and reached remarkable values (> 0.2 mm) under service loads (Fig. 8). In specimens with transverse reinforcement, the anchorage capacity was reached after the complete propagation of the splitting crack along the bar, owing to the favourable effects of the stirrup confining-action. In specimens without transverse reinforcement, an earlier splitting collapse of the anchorage occurred.

- Anchorage capacity increases with the stirrup index of confinement Ω up to an upper bound; in fact, no significant increase of bond strength occurred for $\Omega >$ 0.03-0.04 (Fig. 11a). Anchorage capacity also depends on transverse reinforcement distribution along the section width since stirrup legs placed close to the anchored bars limit splitting crack opening and increase bond capacity.

- Although the transverse reinforcement area was always larger than the minimum value required by EC2, stirrups yielded before reaching the characteristic bond strength $f_{bk,EC2}$ prescribed by the code; in a real beam, this would provoke a reduction of the ultimate load because of an earlier stirrup failure. Moreover, stirrup in specimens with a small amount of transverse reinforcement yielded under service loads (Fig. 10).

A comparison with the values prescribed by building codes evidenced that the bond strength according to Eurocode 2 and ACI 318-95 remarkably underestimated the experimental anchorage capacity for large values of stirrup index of confinement when all the anchored bars are supported by stirrups (Fig. 11a). However, when anchored bars are not placed close to stirrup legs so that a larger splitting crack opening occurs locally, the bond strength prescribed by ACI 318-95 and by EC2 overestimated some experimental results available in the literature (Fig. 11b).

The anchorage capacity of prestressing strands also increases when transverse reinforcement is present along the tendon [30]. Although bond mechanisms in strands differ from ribbed bars, the results here presented provide qualitative information on transverse reinforcement effects on anchorages of prestressing strands. However, because the lack of experimental results, more research should be undertaken in this field.

Finally, with a view to the future, a better understanding of all the aspects related to concrete splitting and transverse reinforcement effects also is required by the latest advances in the field of structural materials. In fact, lightweight and high-strength concretes are particularly sensitive to splitting because of their brittle behaviour as are systems with epoxy coated bars, which induce a larger wedging action on the surrounding concrete.

6 Acknowledgments

This research project was financed by both the Italian National Council for Scientific Research - CNR (national project "Special materials for better structures") and by Valsabbia steelworks "Ferriera Valsabbia" (Odolo, Brescia, Italy). The understanding and cooperation of Mr. Ruggero Brunori (Project Manager) and Mr. Fabrizio Oliva (Project Monitor) of Ferriera Valsabbia, are kindly acknowledged. The authors are also indebted to Prof. Ezio Giuriani and Prof. Alberto Franchi for their useful suggestions, as well as to Mr. Alessandro Coffetti and the technical staff of the laboratory P. Pisa (Brescia University) for their patience and skillfulness in preparing the tests.

References

[1] R. Tepfers. *A Theory of Bond applied to Overlapped Tensile Reinforcement Splices for Deformed Bars*. PhD thesis, Chalmers University of Technology, Goteborg, 1973.

[2] P.G. Gambarova and G.P. Rosati. Bond and Splitting in bar Pull-out: Behavioral Laws and Concrete Cover Role. *Magazine of Concrete Research*, 49(179):99–110, 1997.

[3] E. Giuriani and G.A. Plizzari. Interrelation of Splitting and Flexural Cracks in Reinforced Concrete Beams. *ASCE, Journal of Structural Engineering*, 124(9), 1998.

[4] R. Eligehausen, V.V. Bertero, and E. P. Popov. Local Bond Stress-Slip Relationships of Deformed Bars Under Generalized Excitations: Tests and Analytical Model. Technical Report UCB/EERC-83, Earthquake Engineering Research Center, University of California, Berkeley, California, 1983.

[5] E. Giuriani and G.A. Plizzari. Local Bond-Slip Law after Splitting of Concrete. *Studi e Ricerche, School for the Design of R.C. Structures, Milan University of Technology*, 7:57–118, 1985. in Italian.

[6] G.A. Plizzari, C. Schumm, and E. Giuriani. The Effect of Residual Tensile Strength of Cracked Concrete on the Local Bond-Slip Law after Splitting. *Studi e Ricerche, School for the Design of R.C. Structures, Milan University of Technology*, 9:129–155, 1987.

[7] H.W. Reinhardt and C. Van der Veen. Splitting Failure of a Strain-Softening material due to Bond Stresses. In Alberto Carpinteri, editor, *Applications of Fracture Mechanics to Reinforced Concrete*, pages 333–346, Turin, October 6 1990. Elsevier Applied Science.

[8] P. Balaguru, P.G. Gambarova, G.P. Rosati, and Schumm C.E. Bond of Reinforcing Bars and Prestressing Tendons in HPFRCC Matrices. In A.E. Naaman and H.W. Reinhardt, editors, *Second International Workshop: High-Performance Fiber Reinforced Composities - Volume 2*, pages 325–363, AnnArbor, Michigan, June 11-14 1995. University of Michigan - Dept. of Civil and Environmental Engineering.

[9] R.E. Untrauer and R.L. Henry. Influence of Normal Pressure on Bond Strength. *ACI Journal, Proceedings*, 62(5):577–586, 1965.

[10] R.J. Malvar. Bond of Reinforcement under Controlled Confinement. Technical Report N-1833, Naval Civil Engineering Laboratory, Port Hueneme, California, June 1991.

[11] E. Giuriani, G.A. Plizzari, and C. Schumm. Role of Stirrups and Residual Tensile Strength of Cracked Concrete on Bond. *ASCE, Journal of Structural Engineering*, 117:1–18, 1991.

[12] G.P. Gambarova and E. Giuriani. Discussion of 'Study of the transfer of Tensile Forces by Bond.' by D. H. Jiang, S. P. Shah, and A. T. Andonian. *Proceedings, American Concrete Institute Journal*, 82(3):381–383, 1985.

[13] G.A. Plizzari, E. Marchina, and E. Giuriani. Experimental Study of Splitting and Flexural Cracks in a RC Beam with Overlapped Splices. *RILEM Materials and Structures*, 29:19–27, 1996.

[14] G.A. Plizzari, A.M. Deldossi, and S. Massimo. Experimental Study on Anchored Bars in R.C. Elements with Transverse Reinforcement. *RILEM Materials and Structures*, 29:534–542, 1996.

[15] European Committee for Standardization. *EUROCODE No.2: Design of Concrete Structures - Part 1-1: General Rules and Rules for Buildings-ENV 1992-1-1*. Brussel, 1991.

[16] ACI Committee 318. *Building Code Requirements for Reinforced Concrete, (ACI 318-95)*. American Concrete Institute, Farmington Hills, MI (USA), 1995.

[17] G.A. Plizzari, A.M. Deldossi, and S. Massimo. Experimental investigation on long anchorages confined by transverse reinforcement. Technical Report 5.5/96, Department of Civil Engineering, University of Brescia, Brescia, Italy, 1996. in Italian.

[18] G. Rehm. Ueber die Grundlagen des Verbundes zwischen Stahl und Beton. *Deutcher Ausschuß für Stahlbeton (D.A.f.St)*, 138, 1961. in German.

[19] Comite Eurointernational du Beton. *CEB-FIP Model Code 1990*. C.E.B Bullettins d'Information 213-214, May 1993.

[20] M. Maeda, S. Otani, and H. Aoyama. Effect of Confinement on Bond Splitting Behavior in Reinforced Concrete Beams. *IABSE, Structural Engineering International*, 5(3):166–171, 1995.

[21] S. Morita and S. Fujii. Bond Capacity of Deformed Bars due to Splitting of Surrounding Concrete. In P. Bartos, editor, *Bond in Concrete*, pages 331–352. Applied Science Publishers, London, England, 1982.

[22] T. Kaku, M. Yamada, M. Shibata, and H. Takahashi. Bond Splitting Strength of Simply Supported Reinforced Concrete Beams. *Transactions of the Japan Concrete Institute*, 10:171–176, 1988.

[23] T. Kaku, M. Yamada, and M. Gouraku. Effect of Transverse Reinforcement on Bond Splitting Strength of Reinforced Concrete Beams. *Transactions of the Japan Concrete Institute*, 11:371–378, 1989.

[24] G.E. Warren. *Anchorage Strength of Tensile Steel in Reinforced Concrete Beams.* PhD thesis, Iowa State University, Ames, 1969.

[25] C.O. Orangun, J.O. Jirsa, and J.E. Breen. A reevaluation of Test Data on Development Length and Splices. *ACI Journal*, 74(11):114–122, 1977.

[26] D. Darwin, S.L. McCabe, E.K. Idun, and S.P. Schoenekase. Development Length Criteria: Bars Not Confined by Transverse Reinforcement. *ACI Structural Journal*, 89(6):709–720, 1992.

[27] D. Darwin, Z. Zuo, M.L. Tholen, and E.K. Idun. Development Length Criteria for Conventional and High Relative Rib Area Reinforcing Bars. *ACI Structural Journal*, 93(3):347–359, 1996.

[28] P.G. Gambarova and G.P. Rosati. Bond and Splitting in Reinforced Concrete: Test Results on Bar Pull-out. *RILEM Materials and Structures*, 29:267–276, 1996.

[29] C. Modena, T. Coltro, and G.P. Rossaro. A study of Steel-to-Concrete Bond after Concrete Splitting: Experimental Results at Constant Confinement. *Studi e Ricerche, School for the Design of R.C. Structures, Milan University of Technology*, 10:179–218, 1988. in Italian.

[30] A.J. Bigaj, J.A. Den Uijl, and J.C. Walraven. A Bond Model for Ribbed Bars in HSC and NSC - An Experimental Study. In *4th International Symposium on Utilization of High-strength/ High-performance concrete*, pages 1125–1134, Paris, 1996.

[31] G.A. Plizzari and C. Schumm. On Bond Collapse due to Bar Pull-out and Concrete Splitting. *Studi e Ricerche, School for the Design of R.C. Structures, Milan University of Technology*, 12:81–116, 1990. in Italian.

A Notation

The following symbols are used in this paper:

A_p^*	=	longitudinal-section area of one anchored bar in influence length Δz;
A_{st}	=	cross-section area of the transverse bar leg;
B	=	concrete index of confinement: $B = (b - n_p\phi_p)/(n_p\phi_p)$;
$E_{c,28}$	=	Young's modulus of concrete after 28 days;
F_{max}	=	maximum pull-out load;
K_{tr}	=	transverse reinforcement index according to ACI 318-95;
b	=	cross-section width;
c	=	coefficient for the concrete confining action according to ACI 318-95;
$f_{b,ACI}$	=	bond strength prescribed ACI 318-95 for design;
$f_{b,EC2}$	=	bond strength prescribed by EC2 for design: $f_{b,EC2} = f_{bk,EC2}/\gamma_c$;
$f_{bk,EC2}$	=	characteristic value of the bond strength according to EC2;
f_c'	=	specified cylindrical compressive strength according to ACI 318-95;
$f_{c,cube}$	=	concrete cube strength in compression;
f_{ck}	=	concrete characteristic cylindrical strength in compression according to EC2;
$f_{ck,cube}$	=	concrete characteristic cube strength in compression according to EC2;
$f_{c,28}$	=	concrete cylindrical strength in compression after 28 days;
$f_{ct,28}$	=	concrete cylindrical strength in tension after 28 days;
f_{st}	=	steel tensile strength;
f_{sy}	=	steel yield strength;
f_y	=	specified yield strength for anchored reinforcement according to ACI 318-95;
f_{yt}	=	specified yield strength for stirrups according to ACI 318-95;
l_b	=	anchorage length;
n_p	=	number of anchored bars;
n_{st}	=	leg number of stirrups in the section width;
w_{si}	=	splitting crack opening close to the stirrups (i = 1,2,3);
Δz	=	transverse reinforcement spacing;
Ω	=	stirrup index of confinement: $\Omega = (n_{st}A_{st})/(n_p\phi_p\Delta z)$;
γ	=	coefficient related to the bar diameter according to ACI 318-95;
γ_c	=	concrete safety factor according to EC2;
δ_F	=	free-end slip of the anchored reinforcement;
δ_L	=	loaded-end slip of the anchored reinforcement;
$\delta_{L,P}$	=	loaded-end slip at the maximum load;
σ_P	=	maximum stress in the anchored reinforcement;
σ_{sti}	=	stirrup stresses (i = 1,2,3);
τ	=	average anchored-reinforcement bond stress;
τ_u	=	maximum bond stress;
ϕ_p	=	anchored-bar diameter;
ϕ_{st}	=	transverse-bar diameter.

Contents

List of Figures

List of Tables

Table 1: Geometrical characteristics of the specimens tested.

Specimen	ϕ_{st} [mm]	Ω	ϕ_p [mm]	A_{st1L} [mm^2]	A_{st1R} [mm^2]	A_{st2L} [mm^2]	A_{st2R} [mm^2]	A_{st3L} [mm^2]	A_{st3R} [mm^2]
45NSP1	-	0	20	-	-	-	-	-	-
45NSP2	-	0	20	-	-	-	-	-	-
45S5P1	5*	0.00654	20	17.60	19.29	19.29	19.29	19.29	19.29
45S5P3	5*	0.00654	20**	18.50	19.29	19.29	19.29	19.29	19.29
45S5P4	5*	0.00654	20**	18.40	18.60	18.00	19.29	18.20	19.29
45S6P1	6	0.00942	20	28.39	28.39	28.39	28.39	28.39	28.39
45S6P2	6	0.00942	20	26.90	28.39	28.39	28.39	28.39	28.39
45S6P3	6	0.00942	20**	28.39	26.50	28.39	28.39	28.39	28.39
45S6P4	6	0.00942	20**	26.20	26.00	28.39	26.10	28.39	26.50
45S8P1	8	0.01675	20	42.50	48.77	48.77	48.77	48.77	48.77
45S8P2	8	0.01675	20	40.50	42.50	43.10	48.77	42.90	48.77
45S8P3	8	0.01675	20**	49.60	48.77	48.77	48.77	48.77	48.77
45S8P4	8	0.01675	20**	48.50	48.77	48.77	47.90	48.77	48.70
45S10P4	10	0.02618	20**	73.70	75.71	75.71	72.30	75.71	74.70

* = cold-drawn bars; ** = heat-treated bars.

Table 2: Aggregate composition of concrete.

Diameter $[mm]$	Weight [kg/m^3]	Percentage [%]
0.00÷0.35	229	12.4
0.35÷0.45	39	2.1
0.40÷0.60	51	2.8
0.60÷1.50	223	12
1.50÷2.50	176	9.5
2.50÷3.50	207	11.2
4.00÷6.00	223	12
7.00÷12.0	353	19.1
10.0÷15.0	352	18.9

Table 3: Geometrical and mechanical properties of the reinforcing bars.

Nominal diameter ϕ [mm]	5*	6	8	10	20	20 h.t.
Core diameter D [mm]	4.87	5.47	7.33	9.18	19.0	19.0
Average rib height $a_{m,1}$[mm]	0.27	0.366	0.468	0.505	0.939	1.101
$a_{m,2}$[mm]		0.376	0.424	0.495	0.996	1.098
$a_{m,3}$[mm]		0.357	0.447	0.548	0.999	1.098
Rib inclination β_1	60^o	51^o	53^o	56^o	59^o	59^o
β_2		45^o	43^o	48^o	67^o	53^o
β_3		63^o	63^o	67^o	52^o	69^o
Rib spacing $c_{s,1}$ [mm]	3.5	5.4	6.2	6.55	12	11.6
$c_{s,2}$ [mm]		5.3	6.1	6.65	12.5	11.7
$c_{s,3}$ [mm]		5.3	6.1	6.75	13	11.7
Rib length $l_{r,1}$ [mm]	4.55	11	15	16	35	32.5
$l_{r,2}$ [mm]		12	17	18	33	36
$l_{r,3}$ [mm]		9	13	16	39	30
Related rib area f_R	0.058	0.0615	0.069	0.067	0.0747	0.0733
Yield strength f_{sy} [MPa]	647	535	607	564	536.5	/
Tensile strength f_{st} [MPa]	682	595	677	664	621.5	1265

* = cold-drawn bars - h.t. = heat-treated bars.

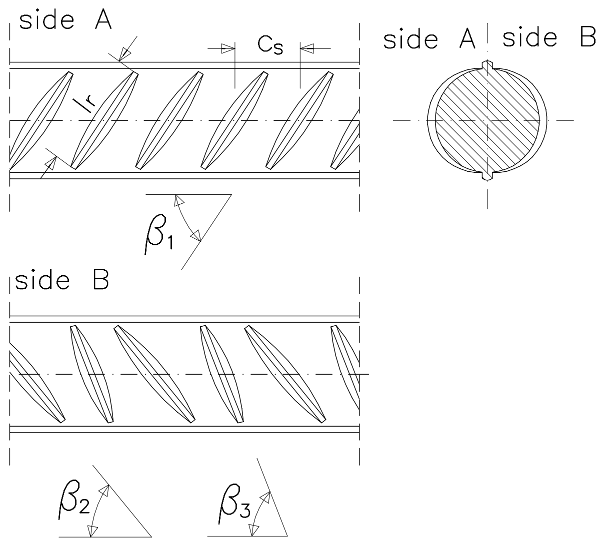

Table 4: Mechanical properties of concrete after 28 days of curing.

Specimen	$f_{c,28}$ [MPa]	$f_{ct,28}$ [MPa]	$E_{c,28}$ [MPa]
45S6P1	41.50	2.60	31100
45S6P2			
45S5P1	24.25	2.80	27263
45S8P1			
45S8P2			
45S6P3	33.95	2.50	29938
45S6P4			
45S8P3			
45S8P4			
45S10P4			
45NSP1	24.90	2.84	29455
45NSP2			
45S5P3	31.49	2.45	28845
45S5P4			

Table 5: Values of peak load F_{max}, loaded-end slip $\delta_{L,P}$, maximum stress σ_P in the anchored bar, bond capacity τ_u and concrete compressive strength $f_{c,cube}$.

Specimen		Age [days]	F_{max} [kN]	$\delta_{L,P}$ [mm]	σ_P [MPa]	τ_u [MPa]	$f_{c,cube}$ [MPa]
45NSP1	right side	29	53.84	0.121	171.4	1.90	28.2
	left side		43.21	0.179	137.5	1.52	
45NSP2	right side	38	46.15	0.243	146.9	1.63	30.6
	left side		53.75	0.146	171.0	1.90	
45S5P1	right side	32	118.92	1.089	378.5	4.20	31.8
	left side		141.83	2.130	451.4	5.01	
45S5P3	right side	48	132.95*	1.128*	423.2	4.70	31.4
	left side		118.50*	0.722*	377.1	4.19	
45S5P4	right side	62	137.51	0.790	437.7	4.86	33.0
	left side		128.38	0.898	408.6	4.54	
45S6P1	right side	22	139.70	1.125	444.6	4.94	29.7
	left side		139.70	0.963	444.6	4.94	
45S6P2	right side	82	118.53*	0.427*	377.3	4.19	36.6
	left side		122.20*	0.430*	389.0	4.32	
45S6P3	right side	27	138.62	1.062	441.2	4.90	29.5
	left side		119.29	0.812	379.7	4.21	
45S6P4	right side	47	125.44	0.848	399.3	4.43	30.3
	left side		139.38	0.882	443.6	4.92	
45S8P1	right side	65	154.95*	1.026*	493.2	5.48	32.8
	left side		136.37*	0.712*	434.0	4.82	
45S8P2	right side	60	144.79*	0.669*	460.9	5.12	32.2
	left side		121.67*	0.684*	387.3	4.30	
45S8P3	right side	40	205.77	1.238	655.0	7.27	28.2
	left side		184.82	1.095	588.3	6.53	
45S8P4	right side	50	~199.35	~1.101	~634.55	~7.05	33.1
	left side		~193.66	~1.180	~616.43	~6.84	
45S10P4	right side	93	261.54	1.500	832.5	9.25	29.1
	left side		183.33	1.187	583.6	6.48	

* = yielding in the sections with strain gauges.

Abstract

In the present research project, long anchorages provided with transverse reinforcement were tested with the aim of studying the confining effects of the stirrups. Particular attention was devoted to gathering detailed data on bar-to-concrete slip, splitting crack propagation and stirrup stresses. To carry out the pull-out tests, a special test set-up was build and the friction between the specimen and the reaction plate was eliminated by resorting to a sophisticated design.

The results show that: 1) the maximum splitting crack opening increased for decreasing transverse-reinforcement diameter size and, under service loads, reached remarkable values; 2) anchorage capacity increases with the stirrup index of confinement Ω up to an upper bound; 3) stirrup in specimens with a small amount of transverse reinforcement yielded under service loads.

A comparison with the values prescribed by building codes evidenced that the bond strength prescribed by both Eurocode 2 and ACI 318-95 code remarkably underestimated the experimental anchorage capacity for large values of stirrup index of confinement.

Keywords

Reinforced Concrete, Bond in R.C., Anchorages, Concrete Splitting, Transverse Reinforcement in R.C..

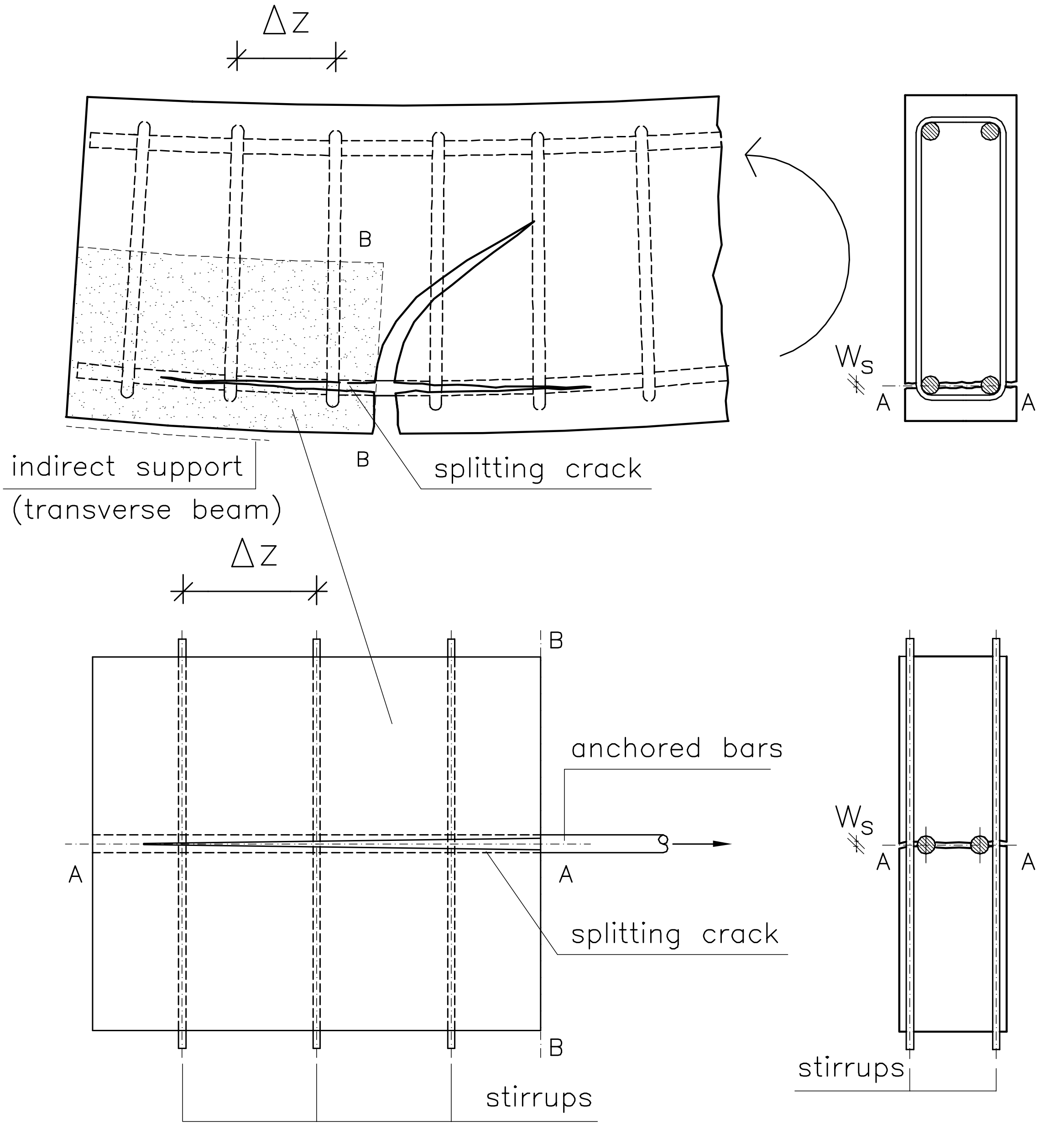

Figure 1: Splitting-crack propagation in anchorages and scheme of the specimen tested.

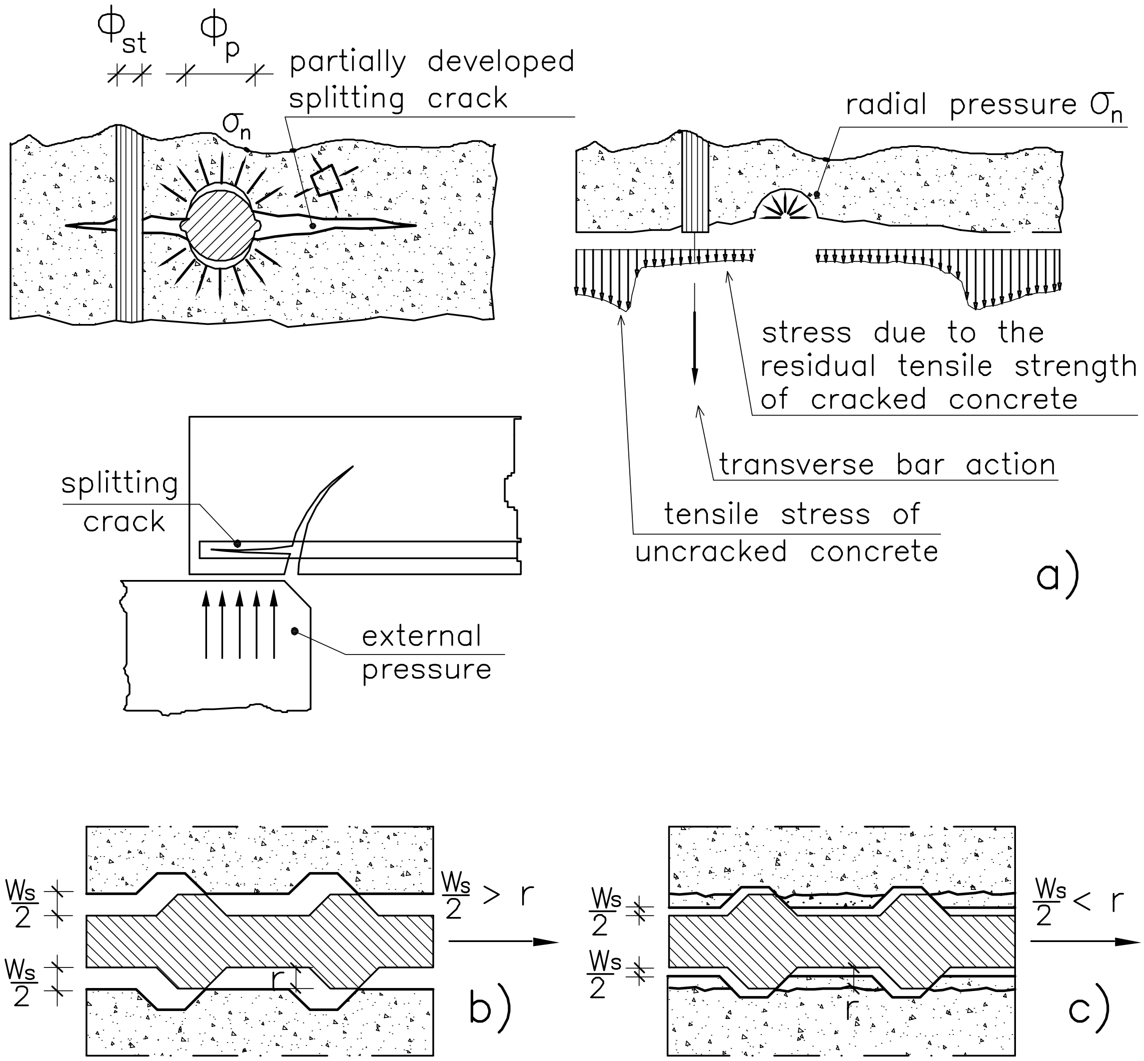

Figure 2: Splitting crack and confining actions around a ribbed bar [11] (a); scheme of local bond failure: "pull-out failure" (b) and "splitting failure" (c) [31].

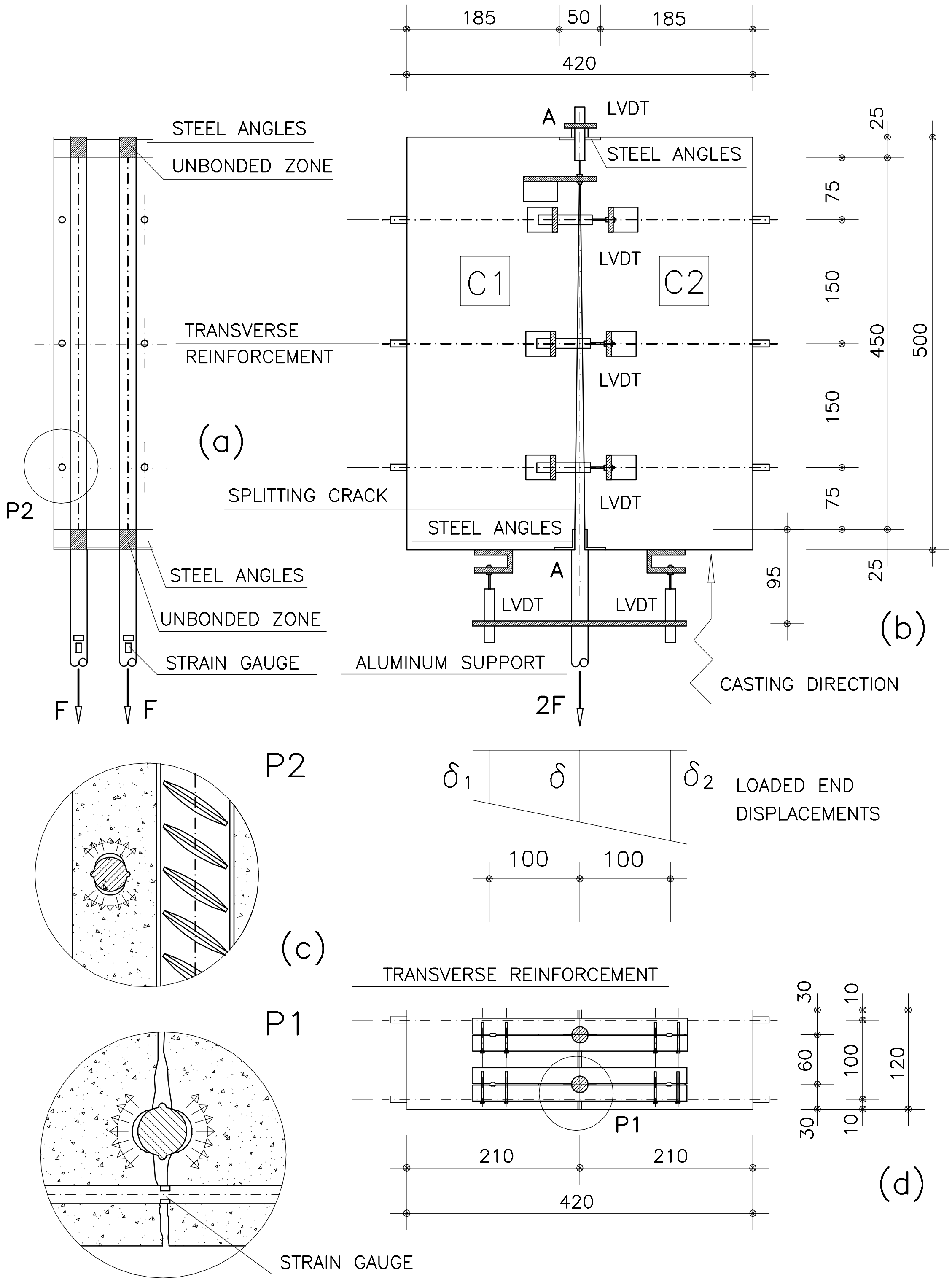

Figure 3: Specimen geometry and instrument placement.

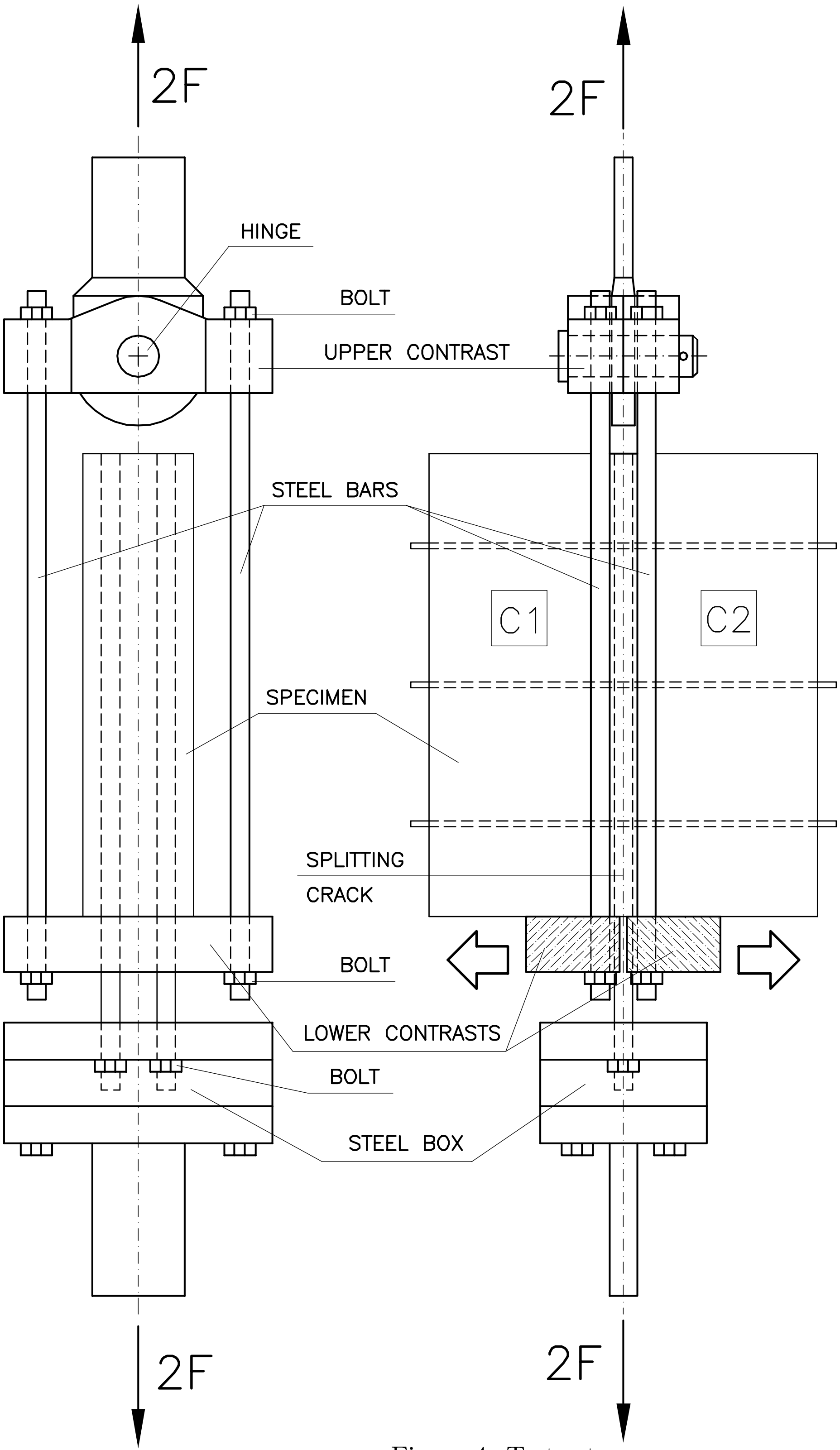

Figure 4: Test set-up.

Figure 5: Typical splitting cracks, as observed in specimens 45S6P4.

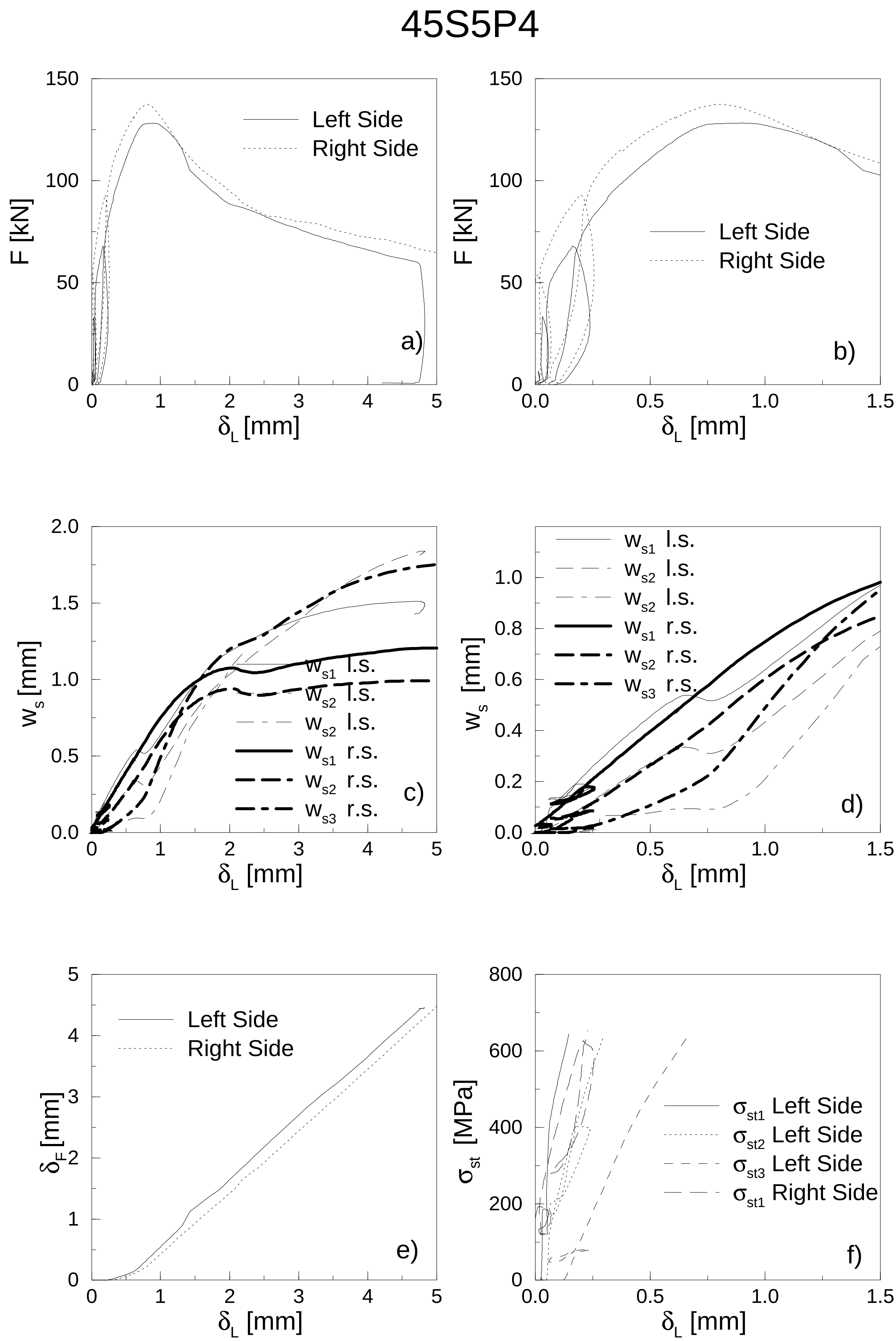

Figure 6: Experimental results obtained from specimen 45S5P4 with 5 mm diameter stirrups.

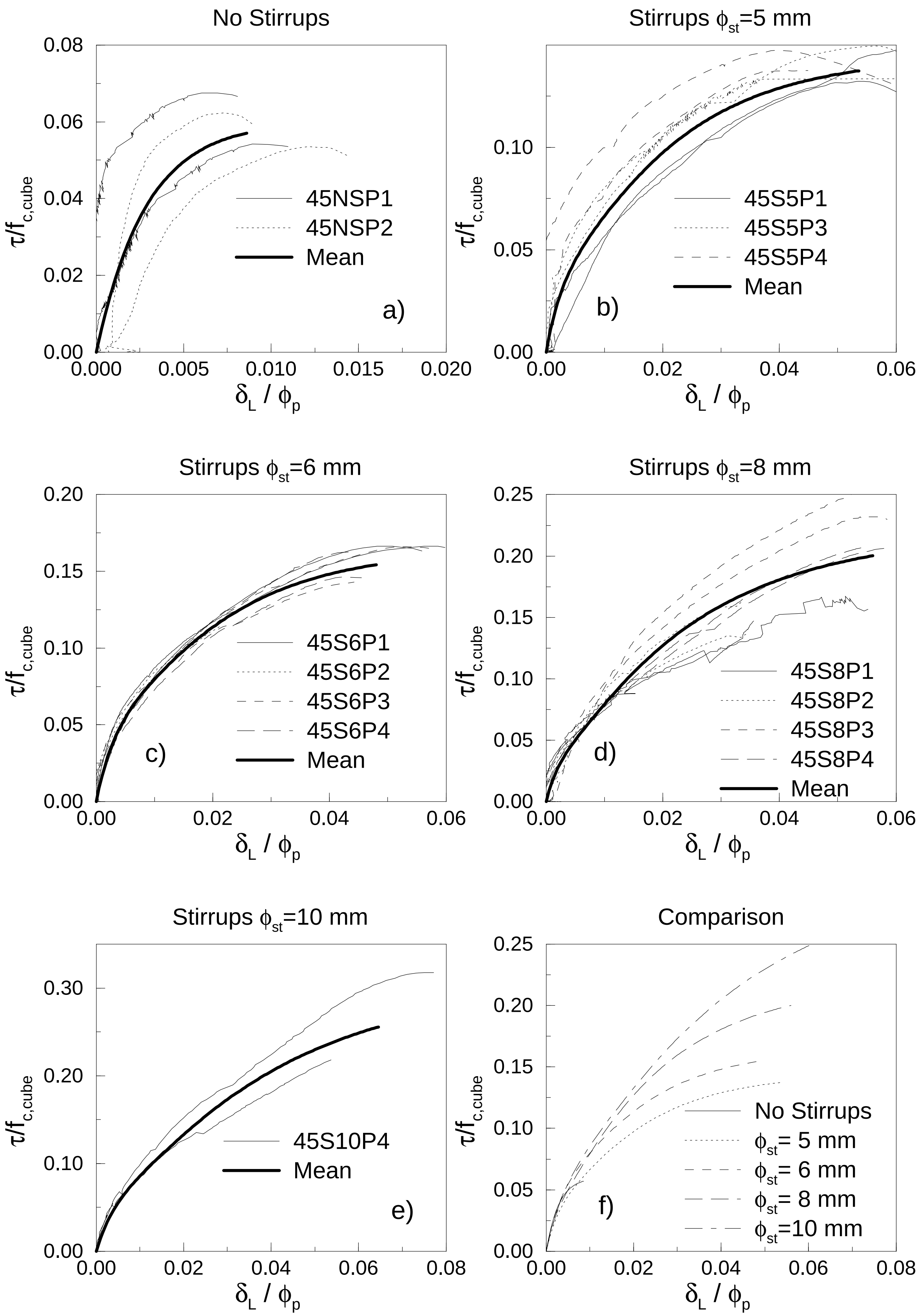

Figure 7: Average bond stress versus loaded-end slip.

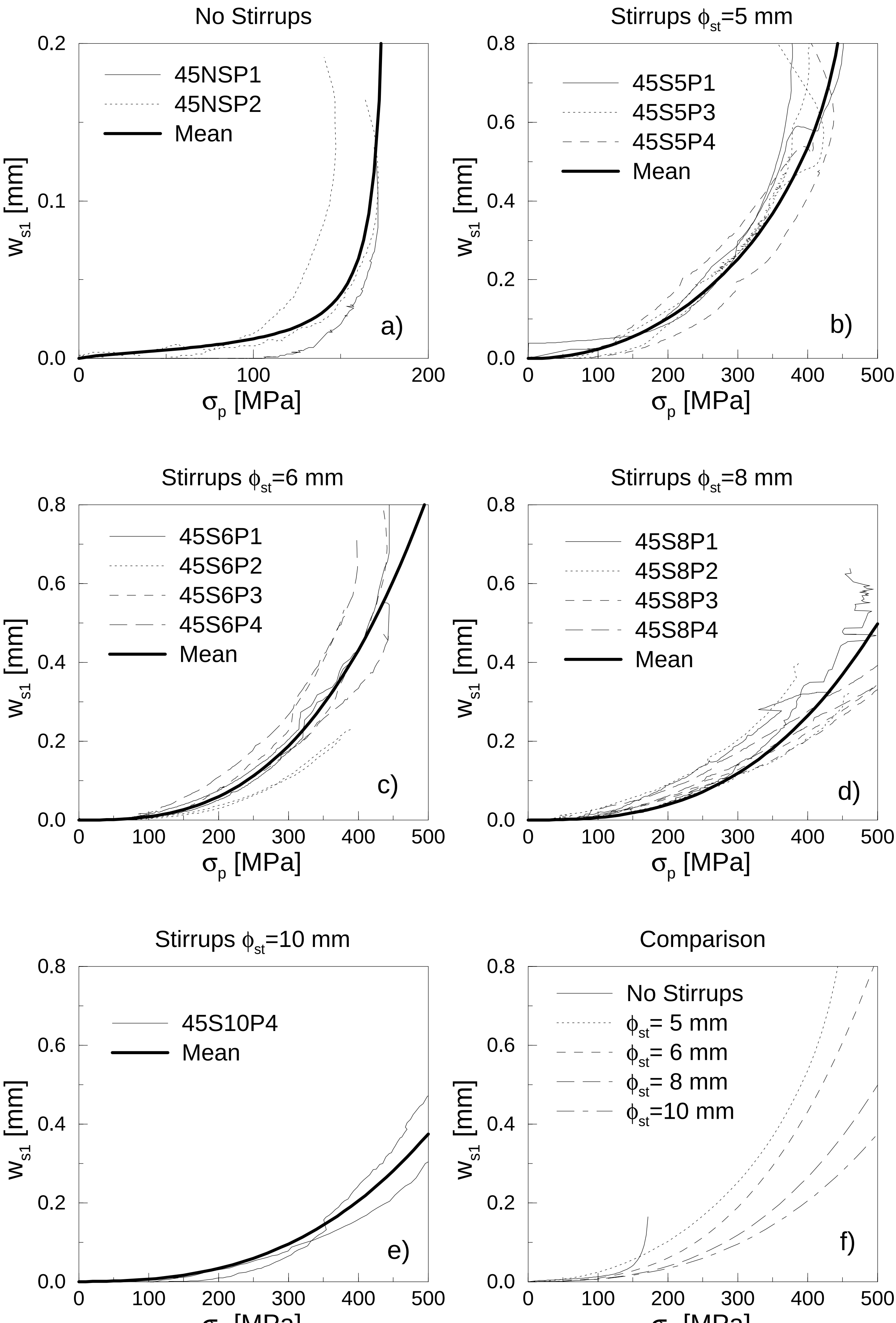

Figure 8: Maximum splitting crack opening at the first-stirrup level versus principal-bar stress.

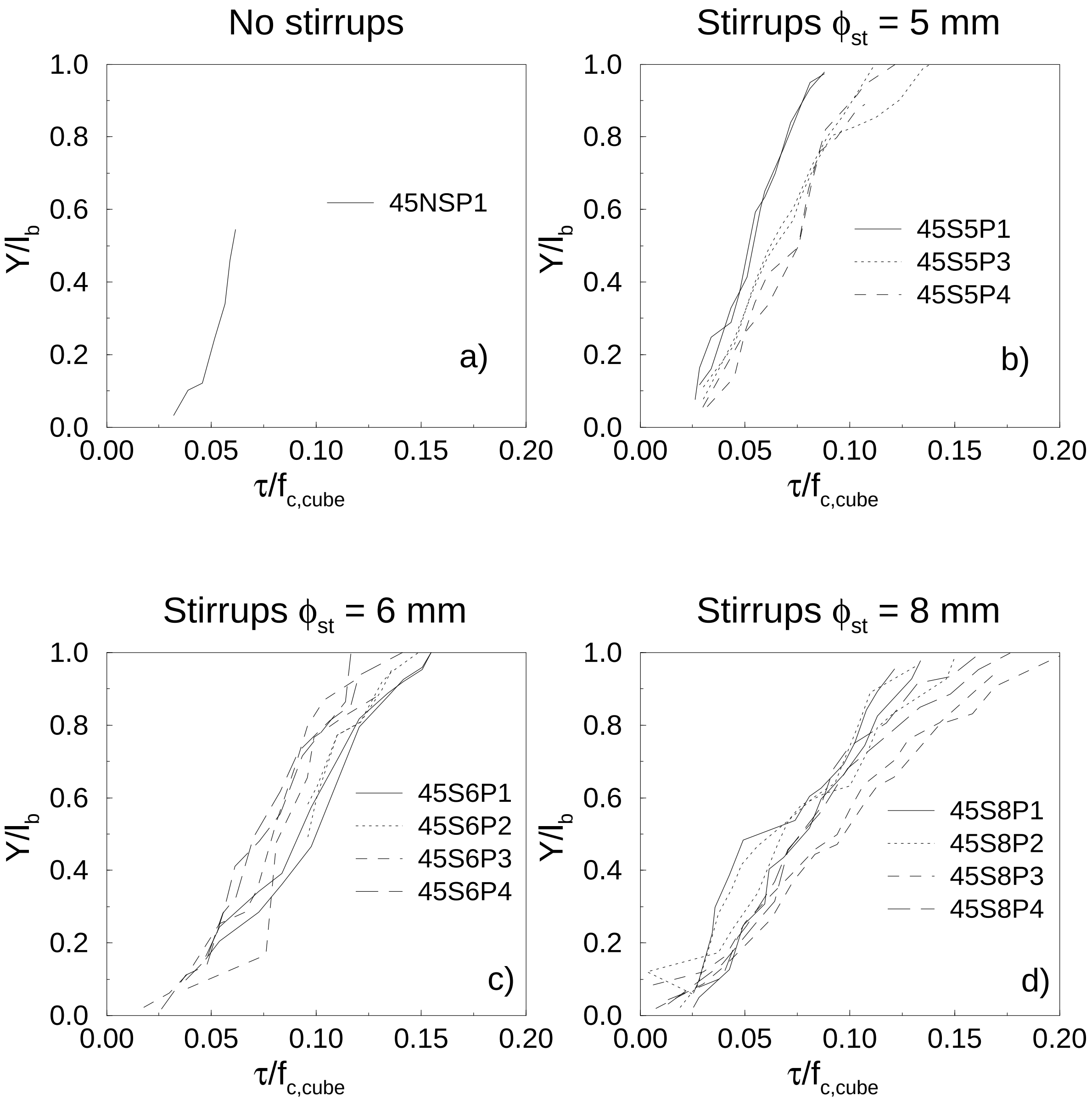

Figure 9: Splitting crack length versus average bond stress.

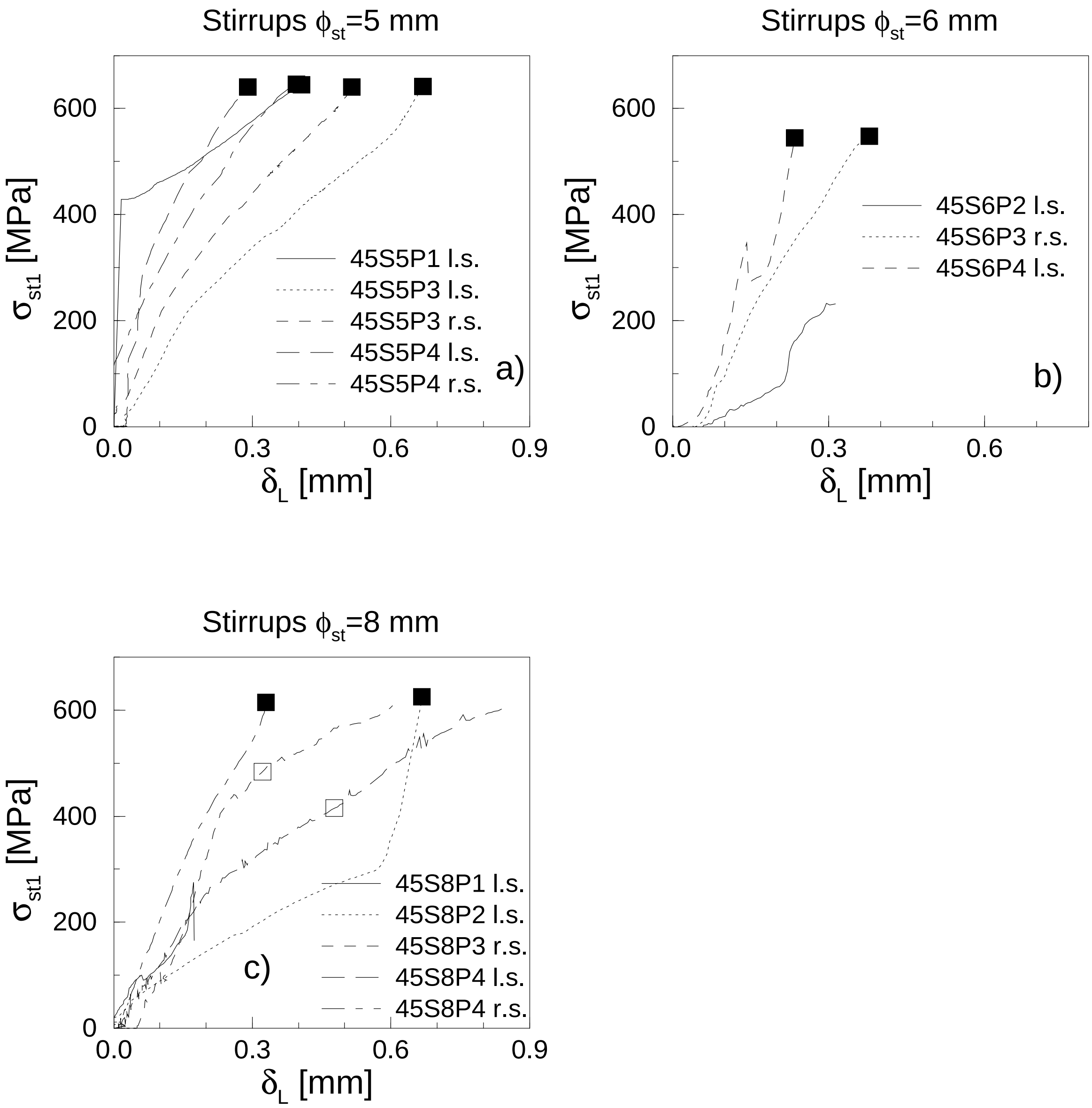

Figure 10: Stress in the stirrup closest to the loaded end of the bar versus loaded-end slip.

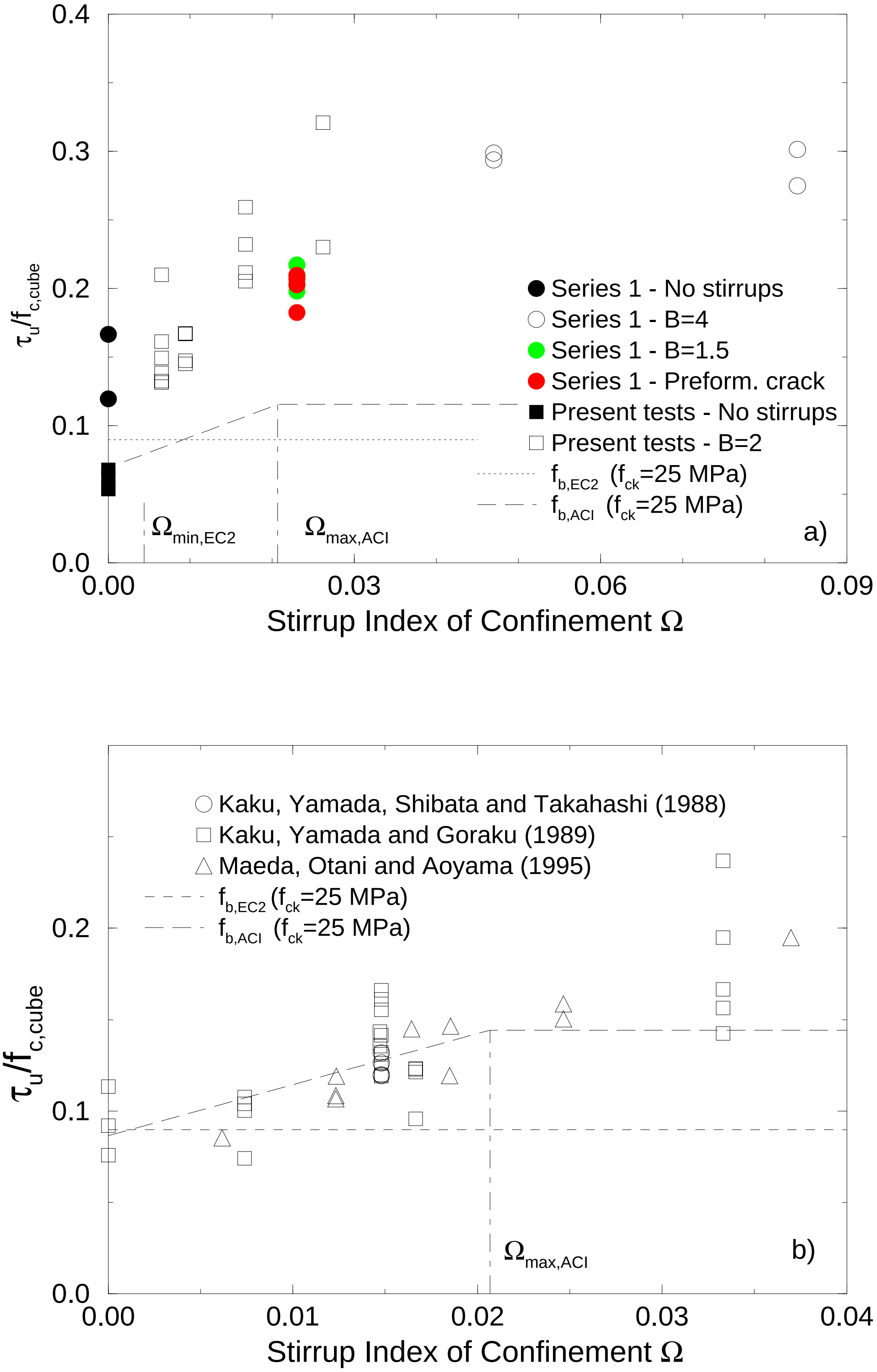

Figure 11: Bond capacity $\tau_u/f_{c,cube}$ versus stirrup index of confinement Ω.